

# Notes

## Concentration Profiles in Densely Tethered Polymer Brushes

Rastislav Levicky,<sup>†</sup> Nagraj Koneripalli,<sup>‡</sup> and Matthew Tirrell\*

Department of Chemical Engineering and Materials Science, University of Minnesota, Minneapolis, Minnesota 55455

Sushil K. Satija

NIST Center for Neutron Research, National Institute of Standards and Technology, Gaithersburg, Maryland 20899

Received December 3, 1997

Revised Manuscript Received February 24, 1998

An assembly of macromolecules tethered by their ends in mutual proximity to a substrate, often referred to as a polymer brush,<sup>1–3</sup> is representative of the structure of a variety of polymer systems such as micelles, star polymers, and adsorbed block copolymer monolayers.<sup>4</sup> This broad relevance to many different polymer systems has spurred much interest in elucidating the factors governing the properties and structure of polymer brushes. The early scaling theory descriptions of polymer brushes by Alexander and deGennes<sup>1</sup> were followed by self-consistent mean field<sup>2,3,5,6</sup> (SCMF) and computer simulation<sup>7,8</sup> studies. These efforts predicted a remarkable stretching of the brush chains perpendicular to the substrate, driven by steric repulsions between polymer segments. For polymer brushes tethered to planar substrates at moderate chain surface densities and immersed in a good solvent, analytical SCMF calculations<sup>2,3</sup> arrived at a parabolic form for the polymer volume fraction  $\Phi(z)$ , where  $z$  is the distance from the substrate. This description has been found to be consistent with several experimental measurements.<sup>9–12</sup> In this note, we address an empirically unresolved issue of the behavior of  $\Phi(z)$  when strong lateral overlap exists between the brush chains.

The polymer brush samples were prepared by spin coating monolayer thick films of anionically synthesized poly(*d*<sub>8</sub>-styrene-*b*-2-vinylpyridine) (dPS-hP2VP) block copolymers from toluene onto 13-mm thick, 100-mm diameter <111> cut polished silicon substrates. Immediately prior to spin coating, the substrates were cleaned for 10 min in a 7:3 mixture of concentrated H<sub>2</sub>SO<sub>4</sub> and aqueous H<sub>2</sub>O<sub>2</sub> (30%) at 120 °C, rinsed in 18 MΩ-cm water, and dried under a nitrogen stream. The spin-coated films were annealed under reduced pressure for 4 days at 185 °C to facilitate the segregation of the hP2VP blocks into a “bottom” layer next to the silicon substrate and the dPS blocks into a “top” layer next to the film/ambient interface. This ordering of the film is

driven by surface-wetting preferences and the incompatibility of the dPS and hP2VP blocks. Exposure of the films to a preferential solvent (toluene or cyclohexane) for dPS caused the dPS layer to swell and form a polymer brush, while the undissolved hP2VP layer anchored the dPS brush to the silicon wafer. We studied four block copolymers of total molecular weights 57, 76, 124, and 216 K, where  $K = 10^3$  g/mol (dPS volume fractions:  $0.50 \pm 0.02$ ; polydispersities: 1.09 to 1.15). The respective sizes of just the dPS blocks were 27, 39, 59, and 103 K. The samples will be hereafter identified by the molecular weight of just the dPS blocks.

Neutron reflectivity measurements were performed on the NG7 reflectometer at the National Institute of Standards and Technology, Gaithersburg, Maryland. The samples were mounted in a temperature-controlled solvent cell,<sup>13</sup> and the reflectivity was measured up to a momentum transfer  $q_z \approx 0.1 \text{ \AA}^{-1}$  ( $q_z = 4\pi \sin \theta/\lambda$ , where  $\theta$  is the angle of incidence and  $\lambda = 4.768 \text{ \AA}$  is the neutron wavelength). The samples were kept under solvent for 30 min prior to initiating measurements. Temperature was controlled to within  $\pm 1$  °C. The first half of each solvent scan was repeated 2 h later (before drying) to confirm data reproducibility and the attainment of swelling equilibrium. In all cases, the two scans superposed. The solvents consisted of a mixture of unlabeled and perdeuterated species in a ratio that produced a scattering length density<sup>14</sup> (SLD) of  $1.4 \times 10^{-6} \text{ \AA}^{-2}$ , close to the hP2VP SLD of  $2.0 \times 10^{-6} \text{ \AA}^{-2}$ . The low contrast between the solvent and the hP2VP anchoring layer enhanced the contribution of the dPS brush (dPS SLD =  $6.4 \times 10^{-6} \text{ \AA}^{-2}$ ) to the reflectivity signal, improving the sensitivity to the brush structure. During data analysis, the experimental reflectivity curves were compared with those calculated from proposed model structures in which the polymer volume fraction profile  $\Phi(z)$  in the brush was represented by

$$\Phi(z) = \Phi(0)(1 - (z/H)^n) \quad 0 \leq z \leq H \quad (1)$$

where  $H$  is the total  $z$ -extent of the brush. Under good solvent conditions and moderate surface chain density, analytical SCMF theory forecasts<sup>2,3</sup>  $n = 2$  corresponding to a parabolic decrease from  $\Phi(0)$  to zero at  $z = H$ . Except for the dPS brush, all other layers were represented by box functions. The sample structure was expressed in terms of its SLD profile, which was then discretized into 3 Å slabs, and the reflectivity was calculated from the recursive Parratt<sup>15</sup> relations. The interfaces between different layers were modeled by locally convoluting the SLD profile with a Gaussian smearing function. Sample structures were iteratively generated, and their reflectivities were compared with experimental ones until the agreement was satisfactory ( $\chi^2 < 3$ ).<sup>16</sup>

The reflectivity data and calculated fits for the 103 K dPS brush under different solvent conditions are

\* To whom correspondence should be addressed.

<sup>†</sup>Presently at the National Institute of Standards and Technology, Bldg. 221/A303, Gaithersburg, Maryland 20899.

<sup>‡</sup>Presently at 3M Corporate Research Science Research Laboratory, 201-2N-19 3M Center, St. Paul, Minnesota 55144.

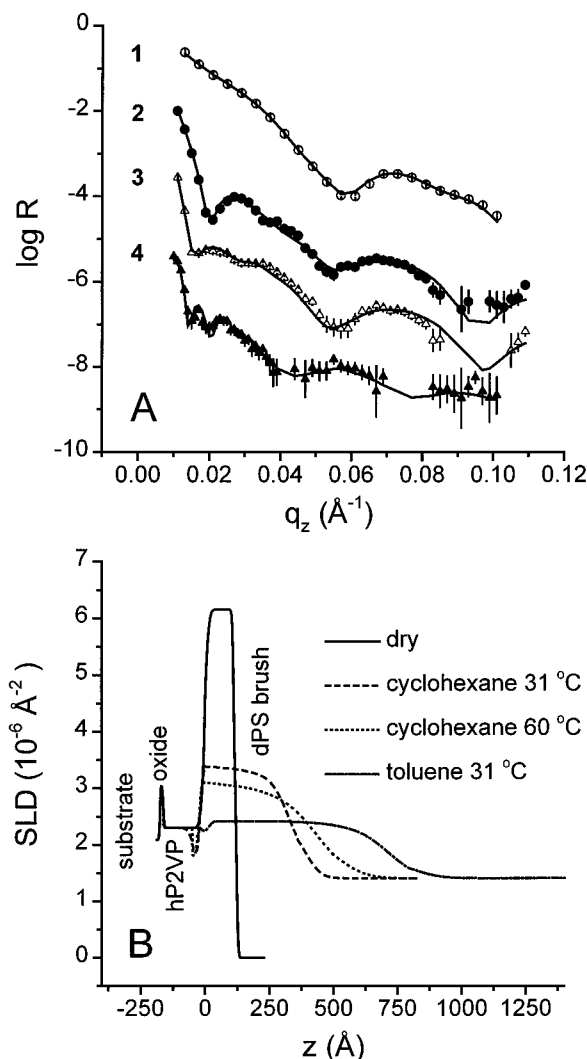


**Figure 1.** (A) Reflectivity data (points) and calculated fits (lines) for the 103 K brush in: (1) dry state, (2) under cyclohexane at 31 °C, (3) under cyclohexane at 60 °C, and (4) under toluene at 31 °C. Starting with the 31 °C cyclohexane data, the curves have been successively shifted down by one order of magnitude for clarity. Data points not used in calculations because of low reflectivity signal have been omitted. (B) The sample structures corresponding to the data and fits in (A).

plotted in Figure 1A. For clarity, the curves have been successively shifted down by one order of magnitude. The SLD profiles corresponding to the calculated fits are shown in Figure 1B. The beginning of the brush is located at  $z=0$ . We first discuss brush structure under toluene, a good solvent for dPS. As illustrated by the calculated reflectivity curves in Figure 2, using the parabolic profile with  $n=2$  led to an inferior fit ( $\chi^2=10$ ) compared with a flatter brush with  $n=5$  ( $\chi^2=1.2$ ). Clearly, the 103 K brush possesses a significantly flatter profile than the classical parabolic prediction.<sup>2,3</sup> In Figure 3A, the 103 K brush profile is compared with the other molecular weight brushes under toluene. The brush SLD profiles have been converted into volume fraction of dPS. Furthermore, the vertical axis has been normalized by  $\Phi(0)$  and the horizontal axis by  $H$ , with the unnormalized profiles shown in the inset. The normalization of the axes overlays the profiles and facilitates comparison of their shapes. The vertical line at  $z=0$  separates the brush bodies (at  $z>0$ ) from the  $\sim 30\text{--}40$  Å wide interfacial “transition region” located

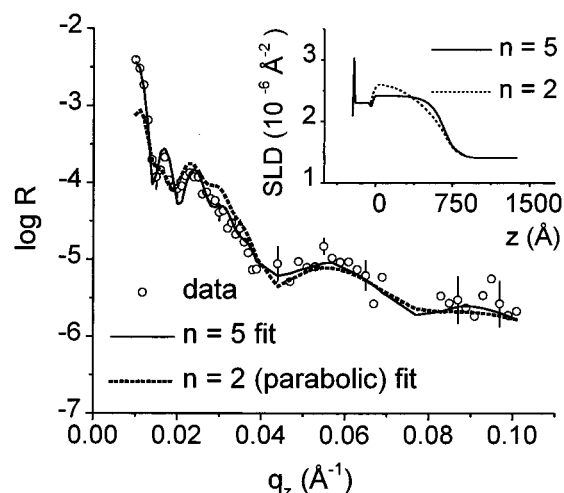


**Figure 2.** Reflectivity data (points) for the 103 K brush in 31 °C toluene, together with calculated reflectivities for a flattened (solid line) and a parabolic (dotted line) brush. For clarity, error bars are shown for every fifth point only. The respective values of the brush exponent  $n$  (eq 1) are indicated. The inset shows the corresponding scattering length density profiles.

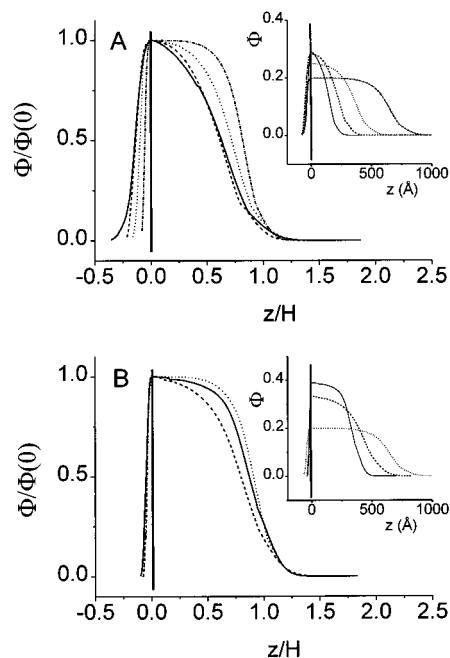


**Figure 3.** (A) Normalized polymer volume fraction profiles in 31 °C toluene for 27 K (solid line), 39 K (dashed line), 59 K (dotted line), and 103 K (dotted-dashed line) brushes. Inset: unnormalized profiles. (B) Normalized polymer volume fraction profiles for the 103 K brush under three different solvent qualities: 31 °C cyclohexane (solid line), 60 °C cyclohexane (dashed line), and 31 °C toluene (dotted line). Inset: unnormalized profiles. The normalized profiles afford a clearer comparison of their shapes.

between the brush bodies and the hP2VP anchoring layer.<sup>17</sup>

The profiles in Figure 3A indicate that higher molecular weight brushes are increasingly flattened. Because all of the profiles were obtained under toluene at 31 °C, effects of solvent quality can be ruled out. If it is not the polymer/solvent interaction that is changing, then the differences in the profiles must stem from the interactions between chains in the brush. For a fixed solvent quality, these interactions are determined by geometrical considerations. A brush can be described

as consisting of self-avoiding walks  $N$  monomers long that are tethered by one end to a surface at a density (chains/area)  $\sigma$ . The condition of self-avoidance limits the configurations available to the chains, and these constraints are reflected in the brush structure. A first-order estimate of the severity of self-avoidance constraints can be obtained by a simple argument. The number of configurational states for a brush of  $P$  self-avoiding chains is designated by  $Z_B$ . The number of configurational states available to  $P$  self-avoiding chains that are isolated from each other is  $z_C^P$ , where  $z_C$  is the number of configurations for one isolated chain. For an athermal polymer/solvent system,  $Z_B/z_C^P = \exp(\Delta S/k)$  where  $\Delta S$  is the decrease in entropy realized by passing from  $P$  isolated chains to the brush state. Although an exact expression for  $\Delta S$  of self-avoiding chains is not available, semidilute scaling theory<sup>1</sup> coarse-grains the brush into a close-packed system of self-avoiding blobs and estimates  $\Delta S/k \sim -P\sigma^*{}^{5/6}$ , where  $\sigma^* \sim \sigma N^{6/5}$ . Accordingly,

$$Z_B^{1/P}/z_C \sim \exp(-\sigma^*{}^{5/6}/k) \quad \sigma^* > 1 \quad (2)$$

By taking the root  $1/P$ , eq 2 has been cast on a "per chain" basis. The overlap surface density  $\sigma^*$  represents the ratio of the area occupied by an isolated chain, which is proportional to the square of the radius of gyration  $R_g \sim N^{3/5}$ , to the area per chain  $\sigma^{-1}$  in the brush. The chains begin to overlap laterally at  $\sigma^* \sim 1$ , with higher  $\sigma^*$  values corresponding to more crowded brushes. Equation 2 suggests that  $\sigma^*$  can be used as a measure of the self-avoidance constraints operative within a brush. For small  $\sigma^*$ ,  $Z_B^{1/P}/z_C \sim 1$ ; but as  $\sigma^*$  increases, the chains overlap more and the intensified self-avoidance constraints result in  $Z_B^{1/P}/z_C \ll 1$ .

We estimated  $\sigma^* = \sigma \pi R_g^2$  using  $R_g$  values for PS in toluene.<sup>18</sup> The respective  $\sigma^*$  values for the 27, 39, 59, and 103 K brushes were 8.0, 15, 19, and 28. In light of eq 2, the  $\sigma^*$  numbers indicate that higher molecular weight samples experienced greater loss of configurational freedom. In the higher molecular weight samples, increased severity of configurational constraints caused a redistribution of polymer segments toward bulk solvent where the chain crowding is less, thus evening out the segment profile. Interestingly, the flatter brushes are actually lower in average polymer concentration (Figure 3A inset) so that the flattening cannot be simply attributed to high segmental density. This result is consistent with identifying the chain overlap  $\sigma^*$ , rather than volume fraction  $\Phi$ , as the measure of self-avoidance constraints (at least within the validity of scaling theory). Previously, comparably flattened profiles were observed in computer simulations<sup>7,8</sup> as well as numerical SCMF calculations that enforce single chain self-avoidance exactly.<sup>6</sup> Experiments<sup>9–12</sup> have been typically conducted at  $\sigma^* < \sim 15$  and have reported parabolic brush shapes, which is in agreement with the parabolic-like profiles of the 27 and 39 K brushes ( $\sigma^* = 8$  and 15, respectively). A parabolic-like profile was also found consistent with reflectivity data from a PS brush in toluene<sup>12</sup> at  $\sigma^* = 24$ ; however, adsorption of brush chains to the substrate surface may have altered the brush profile in that study.<sup>19</sup>

To investigate the effect of solvent quality on the shape of the 103 K brush, reflectivity data were also obtained in cyclohexane at 60 and at 31 °C. The resultant brush profiles are shown in Figure 3B. The

polymer/solvent compatibility progressively worsens passing from toluene to 60 °C cyclohexane to 31 °C cyclohexane, as evidenced by the decrease in brush swelling from  $\sim 780$  Å in toluene to  $\sim 380$  Å in 31 °C cyclohexane (Figure 3B inset). Examination of the normalized profiles reveals an interesting observation – in toluene and in 31 °C cyclohexane, the profiles are flatter than in 60 °C cyclohexane. In toluene, the chains are highly swollen and therefore experience strong lateral overlap, leading to a flatter profile. In contrast, in 31 °C cyclohexane, the profile is flat because increased penalties for polymer/solvent contacts concentrate the polymer into a narrower region next to the substrate. The data in Figure 3B indicate that the interplay of chain overlap and solvent quality can lead to flatter  $\Phi(z)$  in sufficiently good and poor solvents, with rounder  $\Phi(z)$  profiles observed at intermediate solvent qualities. Similar trends are indicated by Monte Carlo simulations of polymer brushes immersed in variable quality solvents.<sup>20</sup> Furthermore, we anticipate that numerical SCMF theories in which the chain configurations are enforced to be strictly self-avoiding<sup>6,21</sup> should exhibit a window of molecular weight, chain surface density, and solvent quality within which such behavior is present.

In conclusion, we have observed flattening of polymer brush concentration profiles with increasing chain overlap. This trend accords with simple arguments based on scaling theory. The flattened profiles underline the importance of self-avoidance constraints in polymer/solvent systems, manifestations of which also give rise to effects such as "sterically enhanced stabilization" observed in colloidal dispersion studies.<sup>22</sup> Additional experiments on strongly overlapped brushes, perhaps employing chains directly polymerized off an initiator-functionalized substrate,<sup>23</sup> would further advance the understanding of the high-density polymer brush regime.

**Acknowledgment.** We thank Igal Szleifer for insightful comments. R.L. is grateful to NSF for financial support through a graduate NSF fellowship. This work was also supported by the Earl E. Bakken Endowment Funds and the Center for Interfacial Engineering, an NSF engineering research center at the University of Minnesota.

## References and Notes

- (a) Alexander, S. *J. Phys. (Paris)* **1977**, *38*, 983. (b) de Gennes, P.-G. *Macromolecules* **1980**, *13*, 1069.
- Milner, S. T.; Witten, T. A.; Cates, M. E. *Macromolecules* **1988**, *21*, 2610.
- Zhulina, E. B.; Pryamitsyn, V. A.; Borisov, O. V. *Polym. Sci. U.S.S.R. (Engl. Transl.)* **1989**, *31*, 205.
- (a) Halperin, A.; Tirrell, M.; Lodge, T. P. *Adv. Polym. Sci.* **1992**, *100*, 31. (b) Milner, S. T. *Science* **1991**, *251*, 905.
- (a) Hirz, S. J. MS Thesis, University of Minnesota, 1986. (b) Wijmans, C. M.; Scheutjens, J. M. H. M.; Zhulina, E. B. *Macromolecules* **1992**, *25*, 2657.
- Carignano, M. A.; Szleifer, I. *J. Chem. Phys.* **1993**, *98*, 5006.
- Murat, M.; Grest, G. S. *Macromolecules* **1993**, *26*, 3108.
- Lai, P.-Y.; Binder, K. *J. Chem. Phys.* **1991**, *95*, 9288.
- Kent, M. S.; Lee, L. T.; Factor, B. J.; Rondelez, F.; Smith, G. S. *J. Chem. Phys.* **1995**, *103*, 2320.
- Field, J. B.; Toprakcioglu, C.; Ball, R. C.; Stanley, H. B.; Dai, L.; Barford, W.; Penfold, J.; Smith, G.; Hamilton, W. *Macromolecules* **1992**, *25*, 434.
- Auroy, P.; Mir, Y.; Auvray, L. *Phys. Rev. Lett.* **1992**, *69*, 93.
- Karim, A.; Satija, S. K.; Douglas, J. F.; Ankner, J. F.; Fetters, L. J. *Phys. Rev. Lett.* **1994**, *73*, 3407.

- (13) Levicky, R.; Koneripalli, N.; Tirrell, M.; Satija, S. K.; Gallagher, P. D.; Ankner, J. F.; Kulasekera, R.; Kaiser, H., submitted for publication in *Macromolecules*.
- (14)  $SLD = \sum \Phi_i SLD_i$ , where  $\Phi_i$  is the volume fraction of species  $i$  and  $SLD_i$  is the value for the pure compound (as calculated from tabulated elemental scattering lengths).
- (15) Parratt, L. G. *Phys. Rev.* **1954**, *95*, 359.
- (16) 
$$\chi^2 = \frac{1}{P} \sum_{i=1}^P \frac{(R_{i \text{ exp}} - R_{i \text{ cal}})^2}{\delta R_i^2}$$
 where  $P$  is the number of data points,  $R_{i \text{ exp}}$  is the experimentally measured reflectivity with standard deviation  $\delta R_i$ , and  $R_{i \text{ cal}}$  is the theoretically calculated reflectivity.
- (17) Two volume fraction profiles can be uniquely obtained from an SLD profile, but in the transition region, three components are present: hP2VP, dPS, and solvent. We assumed a hyperbolic tangent profile for hP2VP to estimate the volume fraction of dPS in the transition region. The details of the transition region are immaterial because the discussion focuses on the shape of the brush body at  $z > 0$ .
- (18)  $R_g = 1.86 N^{0.595}$  Å. Higo, Y.; Ueno, N.; Noda, I. *Polymer J.* **1983**, *5*, 367. Strictly, we should calculate  $\sigma^*$  for the brush in an athermal solvent. However, because the scaling of  $R_g$  with  $N$  is the same for good and athermal solvents, the  $\sigma^*$  values calculated with any good solvent expression for  $R_g$  will be directly proportional to the values in an athermal solvent.
- (19) Karim, A., *personal communication*.
- (20) Lai, P.-Y.; Binder, K. *J. Chem. Phys.* **1992**, *97*, 586.
- (21) Carignano, M. A.; Szleifer, I. *J. Chem. Phys.* **1994**, *100*, 3210.
- (22) Napper, D. H. *Polymeric Stabilization of Colloidal Dispersions*; Academic: New York, 1983.
- (23) Tovar, G.; Paul, S.; Knoll, W.; Prucker, O.; Ruhe, J. *Supramolec. Sci.* **1995**, *2*, 89.

MA9717653